Direct simulation for Reed Wind Instruments

Stefan Bilbao
Music/Acoustics and Fluid Dynamics Group
School of Physics
University of Edinburgh
James Clerk Maxwell Building
Edinburgh EH9 3JZ UK
sbilbao@staffmail.ed.ac.uk

Direct Simulation of Reed Wind Instruments

The synthesis of sound based on physical models of wind instruments has traditionally been carried out in a variety of ways. Digital waveguides (Smith 1986; Scavone 1997; van Walstijn and Campbell 2003; van Walstijn 2007) have been extensively explored, especially in the special cases of cylindrical and conical tubes, in which case they yield an extreme efficiency advantage. A related scattering method, wave digital filtering (Fettweis 1986), is also used to connect waveguide tube models with lumped elements such as an excitation mechanism (Bilbao, Bensa, and Kronland-Martinet 2003) or toneholes (van Walstijn and Scavone 2000). Another body of techniques, closely related to digital waveguides, and based around impedance descriptions, has been developed recently (Guillemain 2004). Other techniques, employing finite-difference approximations to the reed model (as opposed to wave- and scattering-based methods) bear a closer resemblance to the direct simulation methods to be discusssed here (Avanzini and Rocchesso 2002; van Walstijn and Avanzini 2007; Avanzini and van Walstijn 2004). Most of these methods owe a great deal to the much earlier treatment of self-sustained musical oscillators by McIntyre, Schumacher and Woodhouse (1983).

All of these methods rely, to some degree, on simplified descriptions of the resonator (tube). For example, digital waveguides make use of a traveling wave decomposition, accompanied by frequency-domain (impedance or reflectance) characterizations of lumped elements or phenomena such as bell radiation and tone holes. Other methods make use of the Green's function or impulse response of the tube directly (McIntyre, Schumacher and Woodhouse 1983). These methods are, in the end, implemented in the time domain, but the notion of the spatial extent of the tube is suppressed: The system is viewed in an input–output sense. When it comes to sound synthesis, however, it is not clear that it is necessary to do so; once one has arrived at a satisfactory model of a musical instrument, written as a time-space partial-differential-equation (PDE) system (for the resonator) coupled to ordinary differential equations (ODEs, the excitation element and a radiation boundary condition), one may proceed directly to a synthesis algorithm without invoking any notion of frequency, impedance, wave variables, or reflectance, or otherwise making any hypotheses about the dynamics of the air in the tube. Though one of course loses the powerful analysis perspective mentioned previously, the treatment of the resonator becomes independent of any particular bore profile, and the system as a whole is now much more amenable to interesting extensions involving, e.g., time-varying and nonlinear effects which do indeed play a role in wind instruments, and which are not easily approached using impedance or scattering concepts.

In the present case, concerned with audio synthesis (and thus efficiency), the model remains one-dimensional. Standard numerical techniques, and, in particular, finite-difference schemes, have been applied (infrequently) to acoustic tube modeling for some time, especially in the case of speech synthesis (see, e.g., the recent paper by van den Doel and Ascher 2008 and the much older but prescient and comprehensive treatment of Portnoff 1973). Finite-difference schemes have also been applied in multi-dimensional spaces, in the setting of acoustical analysis of wind instruments, though generally not directly for synthesis (e.g., Nederveen 1998; Noreland 2002).

In this article, a standard model of a reed wind instrument is presented first, followed by the development of a finite-difference time-domain algorithm, including some discussion of implementation details, such as the operation count and computability issues. Connections to toneholes are then introduced, followed by simulation results.

This article appeared, in a modified form, at a recent conference (Bilbao 2008), and also forms the basis for a section in a new text (Bilbao 2009).

Computer Music Journal, 33:4, pp. 43–55, Winter 2009

Figure 1. Acoustic tube of variable cross-sectional area S(x).

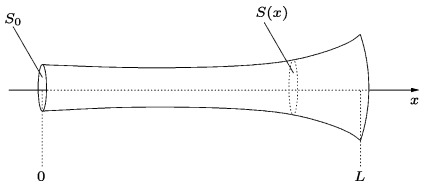

Figure 2. Pressure and flow variables in a reed instrument mouthpiece.

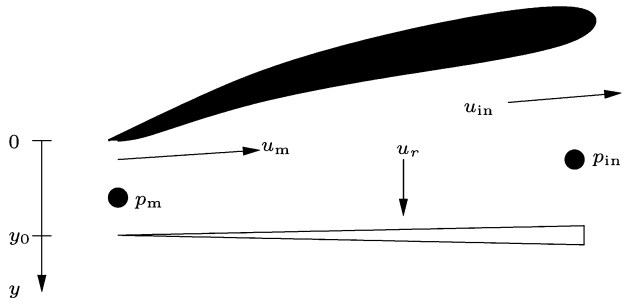

A Standard Wind Instrument Model

Instrument Body

A standard model of one-dimensional linear wave propagation in an acoustic tube (Morse and Ingard 1968) is given by the following set of equations:

$$\frac{\rho}{S}u_t = -p_x \quad \frac{S}{\rho c^2}p_t = -u_x \quad x \in [0, L] \tag{1}$$

Here, $u(x, t)$ and $p(x, t)$ are the volume velocity and pressure, respectively, at position x, and at time t, and subscripts t and x refer to time and space differentiation, respectively. ρ and c are the density and wave speed, respectively, $S(x)$ is the tube cross-sectional area (or rather, the area of an isophase surface of the pressure distribution in the tube; see Benade and Jansson 1974) at position x, and L is the length of the tube (see Figure 1). This system is often condensed into a single second-order system, known as Webster's equation (Fletcher and Rossing 1991):

$$S\Psi_{tt} = c^2(S\Psi_x)_x \quad x \in [0, L] \tag{2}$$

in terms of a velocity potential $\Psi(x, t)$, related to the pressure p and volume velocity u by $p = \rho\Psi_t$ and $u = -S\Psi_x$. Such an equation is the starting point for various speech-synthesis algorithms (Rabiner and Schafer 1978), including the Kelly-Lochbaum model (Kelly and Lochbaum 1962). This model results from many simplifying assumptions, the most important of which are linearity, relatively slow variation in $S(x)$ and the size of $S(x)$ relative to audio wavelengths, and losslessness. For more comments on these assumptions (some more justifiable than others), see the conclusion of this article.

It is useful to dimensionally reduce the problem, by introducing the variables $x' = x/L$, $\Psi' = \Psi/cL$, as well as a dimensionless area function $S' = S/S_0$, where S_0 is a reference surface area, such as $S_0 = S(x = 0)$. This leads, after substitution into Equation 1 and removal of primes, to

$$S\Psi_{tt} = \gamma^2(S\Psi_x)_x \quad x \in [0, 1] \tag{3}$$

where $\gamma = c/L$ is a constant with dimensions of frequency. Initial conditions for the system may be set to zero, and proper boundary conditions (one required at each end of the domain) follow from the consideration of the reed excitation and bell radiation, to be discussed shortly.

Reed Mechanism

A slightly non-standard model of reed vibration can be given as follows (see Figure 2). For a one-mass model, the reed displacement behaves according to

$$\ddot{y} + 2\sigma_0\dot{y} + \omega_0^2(y - H_0) - \frac{\omega_1^{\alpha+1}}{H_0^{\alpha-1}}(|[y]^-|)^\alpha = -\frac{S_{\text{r}}p_\Delta}{M_{\text{r}}} \tag{4}$$

$y(t)$ is here the displacement of the reed relative to an equilibrium position y_0, S_r an effective surface area of the reed, M_r is the reed mass, ω_0 the resonant frequency, and σ_0 a damping parameter. Dots above variables signify total time differentiation. The term involving the coefficient ω_1 models the collision of the reed with the mouthpiece. It acts as a one-sided repelling force, modeled as a power-law nonlinearity, of exponent α, and becomes active when $y < 0$. Here, $[y]^- = (y - |y|)/2$, and the reed displacement y is permitted to be negative. This term, inspired by collision models used in hammer-string dynamics (Chaigne and Askenfelt 1994), is the sole distinguishing feature of the model, which

is otherwise identical to that which appears in the literature (Kergomard, Guillemain, and Voinier 2005; Kergomard 1995; Tachibana and Takahashi 2000; Dalmont, Gilbert, and Ollivier 2003; and Avanzini and van Walstijn 2004).

This oscillator is driven by the pressure difference p_Δ, given by

$$p_\Delta = p_\mathrm{m} - p_\mathrm{in}$$

where $p_\mathrm{m}(t)$ is the mouth pressure, and $p_\mathrm{in}(t)$ the pressure at the entrance to the acoustic tube. Through Bernoulli's law, the pressure difference may be related to the flow in the mouthpiece u_m by

$$u_\mathrm{m} = w[y]^+ \sqrt{\frac{2|p_\Delta|}{\rho}} \mathrm{sign}(p_\Delta) \tag{5}$$

where w is the width of the reed channel. The flow is nonzero only when the reed is not in contact with the mouthpiece, or when $y > 0$. As such, the quantity $[y]^+$ is given by $[y]^+ = (y + |y|)/2$. Neglected here is an inertia term (see, e.g., Fletcher and Rossing 1991). From a numerical standpoint, the square root dependence of flow on velocity could be generalized to a power law (Backus 1963) with few resulting complications in the discretization procedure to be outlined subsequently.

The flow variables are related by a conservation law

$$u_\mathrm{in} = u_\mathrm{m} - u_\mathrm{r}$$

where u_in is the flow entering the acoustic tube, and where u_r is related to reed displacement y by

$$u_r = S_\mathrm{r} \dot{y}$$

It is useful to introduce scaled variables as follows:

$$y' = \frac{y}{H_0} - 1 \quad p'_\cdot = \frac{p_\cdot}{\rho c^2} \quad u'_\cdot = \frac{u_\cdot}{cS_0}$$

Here, $p_\cdot$ and $u_\cdot$ indicate any pressure or flow variables, which, when inserted in the previous equations (and primes subsequently removed) lead to the system:

$$\ddot{y} + 2\sigma_0 \dot{y} + \omega_0^2 y = -\mathcal{Q} p_\Delta + \omega_1^{\alpha+1} (|[y+1]^-|)^\alpha \tag{6a}$$

$$p_\Delta = p_\mathrm{m} - p_\mathrm{in} \tag{6b}$$

$$u_\mathrm{m} = \mathcal{R}[y+1]^+ \sqrt{|p_\Delta|} \mathrm{sign}(p_\Delta) \tag{6c}$$

$$u_\mathrm{in} = u_\mathrm{m} - u_\mathrm{r} \tag{6d}$$

$$u_\mathrm{r} = \mathcal{S} \dot{y} \tag{6e}$$

where

$$\mathcal{Q} = \frac{\rho c^2 S_\mathrm{r}}{M_\mathrm{r} H_0} \quad \mathcal{R} = \sqrt{2} \frac{w H_0}{S_0} \quad \mathcal{S} = \frac{S_\mathrm{r} H_0}{c S_0} \tag{7}$$

Note that higher-order effects of the time variation of H_0 (which is possible during play and is generally quite slow) are neglected here, as in previous treatments of the reed system (Kergomard, Guillemain, and Voinier 2005). Slow variation in H_0 can be introduced here through a function $H_0(t)$; notice that it affects all of the parameters $\mathcal{Q}$, $\mathcal{R}$ and $\mathcal{S}$.

It should be clear that in a connection with the acoustic tube described by Equation 3, it must be true that

$$\Psi_t(0,t) = \gamma p_\mathrm{in}(t) \quad \Psi_x(0,t) = -u_\mathrm{in}(t) \tag{8}$$

Bell Radiation

One boundary condition is required for Webster's equation (Equation 3) at the bell termination at $x = 1$. Normally, in the musical acoustics literature (e.g., Fletcher and Rossing 1991; Atig, Dalmont, and Gilbert 2004), one employs the standard radiation impedance result for an unflanged tube. Often, this is given, in the low-frequency limit, in a polynomial form obtained through a series approximation (Fletcher and Rossing 1991; Atig, Dalmont, and Gilbert 2004). Although this is fine for analysis purposes, positive realness (Belevitch 1968)—and thus passivity—is lost, and numerical instabilities can arise in simulation. It is thus better, in this context, to make use of a rational and positive real approximation to the radiation impedance (see, e.g., the form given in Rabiner and Schafer 1978), leading to the following relationship between scaled pressure and velocity at $x = 1$:

$$\Psi_x(1,t) = -\alpha_1 \Psi_t(1,t) - \alpha_2 \Psi(1,t) \tag{9}$$

In the case of an unflanged tube, the constants α_1 and α_2 take on the values:

$$\alpha_1 = \frac{1}{4(0.6133)^2\gamma} \quad \alpha_2 = \frac{L}{0.6133\sqrt{S_0 S(1)/\pi}} \tag{10}$$

The term with coefficient α_2 corresponds to the reactive part of the radiation impedance, and that with coefficient α_1 to the resistive part. One could go much further here, and develop boundary conditions which model radiation to higher accuracy (thus requiring more state), but the positive realness criterion must continue to be enforced (i.e., a higher order polynomial series approximation to the radiation impedance will lead to the potential for active behavior, and thus numerical instability in simulation). Positive realness of an impedance corresponds directly to bounded realness for the associated reflectance, a quantity which is probably better known to musical acousticians.

A Simple Finite-Difference Scheme

There are many possible choices of finite-difference schemes for Webster's equation, but, interestingly, the simplest possible choice is, in almost all respects, the best (see the section entitled "Dispersion, Accuracy and Mode Tunings"). A grid function Ψ_l^n for integer l, with $0 \leq l \leq N$, and $n \geq 0$, is an approximation to $\Psi(x, t)$ at locations $(x = lh, t = nk)$, where h and k are the spacing between adjacent grid points and time step, respectively (see Figure 3). k is related to the sample rate f_s by $k = 1/f_s$—in audio synthesis applications, k is normally chosen a priori. A simple scheme is of the following form:

$$\Psi_l^{n+1} = m_l^{(-)}\Psi_{l-1}^n + m_l^{(0)}\Psi_l^n + m_l^{(+)}\Psi_{l+1}^n - \Psi_l^{n-1} \tag{11}$$

where the Courant number λ is defined as $\lambda = k\gamma/h$, and where the scheme coefficients are given by

$$m_l^{(-)} = \frac{2\lambda^2(S_l + S_{l-1})}{S_{l-1} + 2S_l + S_{l+1}}$$

$$m_l^{(0)} = 2 - 2\lambda^2$$

$$m_l^{(+)} = \frac{2\lambda^2(S_l + S_{l+1})}{S_{l-1} + 2S_l + S_{l+1}}$$

Figure 3. Computational grid for finite difference scheme (Equation 11) for Webster's equation, coupled to a reed mechanism. At an interior point, the computational dependency of the scheme at a given grid point is indicated by the set of black points with accompanying arrows.

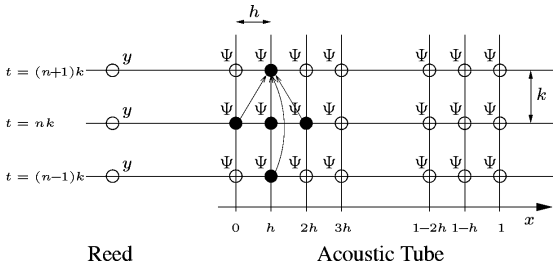

where $S_l \triangleq S(lh)$, and where λ, the Courant number, is given by $\lambda = \gamma k/h$. In implementation, the coefficients may be precomputed, with minimal effort (see Figure 3).

A necessary condition for numerical stability is

$$\lambda \leq 1 \tag{12}$$

This is the familiar Courant-Friedrichs-Lewy condition (Courant, Friedrichs, and Lewy 1928; Strikwerda 1989), arrived at through energy techniques (and not frequency or von Neumann analysis, which is not generally applicable to problems with spatial variation; see Bilbao 2009). Note that the condition is independent of the variation in S itself, simplifying implementation somewhat. In particular, for a given time step k, it is easiest to choose the grid spacing h so as to divide the unit interval into an integer number N of parts, and it is also important that Equation 12 be satisfied as near to equality as possibility. This leads to the choice

$$N = \text{floor}(1/\gamma k) \quad h = 1/N$$

Notice that one could choose a smaller value for N, leading, apparently, to reduced computational costs (i.e., fewer grid values must be computed). Such a choice, though it has been made by some in the context of speech synthesis (see, e.g., van den Doel and Ascher 2008), leads to severe dispersion, and bandlimiting of the output (see the next section for more on this).

The updating of Ψ, according to Equation 11, necessarily requires a boundary condition at either end; these settings will be discussed shortly.

The scheme in Equation 11 can be shown to be equivalent to scattering forms commonly encountered in physical modeling sound sysnthesis; when $\lambda = 1$, it reduces to the Kelly-Lochbaum

Figure 4. A tube profile, and comparisons between exact and numerical modal frequencies resulting from the use of the scheme of Equation 11, running at 44.1 kHz, and for a value of λ chosen as close to 1 as possible. At top, a tube profile grossly characteristic of a wind instruments with a value of $\gamma = 600$. A zero-velocity (Neumann) condition is used at the tube's left end, and a zero-pressure (Dirichlet) condition at its right end.

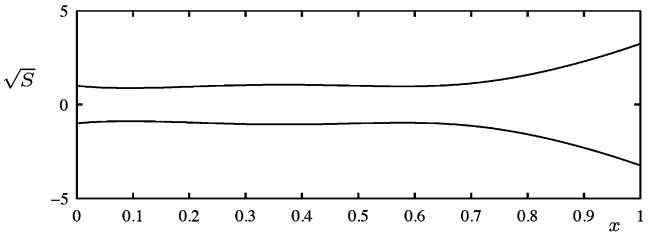

Mode #	Exact Freq. (Hz)	Scheme (11) Freq. (Hz)	Scheme (11) Cent Dev.
1	194.17	194.21	0.34
2	550.89	550.69	-0.63
3	788.08	787.78	-0.65
4	1068.67	1068.50	-0.28
12	3456.35	3455.33	-0.51

model, and if, furthermore, S is constant, it reduces further to the digital waveguide (see Bilbao 2009 for more details).

Dispersion, Accuracy and Mode Tunings

Before proceeding to the case of a complete wind instrument, it is worth taking a look at the behavior of the scheme in Equation 11 on its own, especially with regard to the important issue of accuracy. Equation 11 is formally second-order accurate; one might assume, then, that numerical dispersion (and thus misplacement of modal frequencies) will be a major concern (Strikwerda 1989), as it can be for simulations for other systems in musical acoustics (such as, e.g., the transverse vibration of bars; Bilbao 2009). In fact, though, the formal order of accuracy only refers to the behavior of the scheme in the low-frequency limit; the accuracy of the scheme is extremely good, over the whole range of audio frequencies, even for relatively exotic choices of the bore profile.

Consider, for example, the case of the tube terminated by a zero-velocity condition at $x = 0$, and a zero-pressure condition at $x = 1$ (corresponding, roughtly, to a wind instrument configuration). One finds, using Equation 11, that the modal frequencies of the tube converge very rapidly to their exact values, so that even at a typical audio sample rate (such as 44.1 kHz), the error is far below the threshold of human audio perception (see Figure 4 for some typical values).

In mainstream applications, better accuracy is obtained by using more-involved differnce approximations. In the case of Webster's equation, however, higher-order accurate approximations will tend to degrade accuracy. The explanation of this apparent paradox is that the discretization errors in the temporal and spatial second-order approximations in Equation 11 lead to a rather delicate cancellation. (For much more on this topic, see the literature on so-called modified equation methods, e.g., Shubin and Bell 1987.)

Some comments are in order in this point. First, to obtain this very accurate behavior, the condition in Equation 12 must be satisfied as close to equality as possible.) This means choosing the number of grid points N as large as possible. From the point of view of computational complexity, one must thus be wary of the temptation to choose a smaller N, to save on the total operation count; if one does, numerical dispersion, and, what is worse, a severe bandlimiting of the resulting audio output will result (see, e.g., the results shown in van den Doel and Ascher 2008, where even at an audio sample rate, the output is bandlimited to far below the Nyquist). The issue of truncation is a distinction between difference methods and scattering methods such as waveguides: waveguides under truncation exhibit a slight detuning of modal frequencies, which can be corrected with recourse to fractional delay filters (Välimäki and Karjalainen 1995); difference schemes do not exhibit this detuning, but rather a loss of bandwidth, which is typically very small if the stability condition is satisfied near equality (at 44.1 kHz, in a worst-case scenario for wind instruments, output is bandlimited to approximately 20 kHz).

Scheme for the Reed System

For the reed system given in Equation 6, consider the following scheme:

$$\frac{1}{k^2}(y^{n+1} - 2y^n + y^{n-1}) + \frac{\sigma_0}{k}(y^{n+1} - y^{n-1}) + \frac{\omega_0^2}{2}(y^{n+1} + y^{n-1}) + \frac{\omega_1^{\alpha+1}}{2}|[y^n + 1]^-|^{\alpha-1}(y^{n+1} + y^{n-1}) = -\mathcal{Q}p_\Delta^n \quad (13a)$$

$$p_\Delta^n = p_\mathrm{m}^n - p_\mathrm{in}^n \tag{13b}$$

$$u_\mathrm{m}^n = \mathcal{R}[y^n + 1]^+ \sqrt{|p_\Delta^n|}\,\mathrm{sign}(p_\Delta^n) \tag{13c}$$

$$u_\mathrm{in}^n = u_\mathrm{m}^n - u_\mathrm{r}^n \tag{13d}$$

$$u_\mathrm{r}^n = \frac{\mathcal{S}}{2k}(y^{n+1} - y^{n-1}) \tag{13e}$$

Here, the functions y, u_m, u_r, u_in, p_m, p_in, and p_Δ have been approximated by time series, with time step k. p_m, in particular, is assumed to be a known input control signal, and p_in and u_in will be related to values of the grid function Ψ over the problem interior. Worth noting here is the approximation to the stiffness term (with coefficient ω_0^2) and the collision term (with coefficient $\omega_1^{\alpha+1}$), both of which make use of semi-implicit discretizations. Such implicit approximations, when applied to lumped systems such as the reed, significantly ease stability requirements, and, as long as the unknown value of the grid function appears linearly (as it does here) still allow for fully explicit updating (see the section entitled "Explicit Updating").

Numerical Coupling to the Reed System

To couple the scheme in Equation 11 to that of Equation 13 for the reed, numerical boundary conditions corresponding to the conditions in Equation 8 are necessary; here are particularly well-behaved choices:

$$p_\mathrm{in}^n = \frac{1}{2\gamma k}\left(\Psi_0^{n+1} - \Psi_0^{n-1}\right) \quad u_\mathrm{in}^n = -\frac{1}{2h}\left(\Psi_1^n - \Psi_{-1}^n\right) \tag{14}$$

The second condition refers to a value of the grid function Ψ_l at a virtual location $l = -1$.

After some algebra, the system in Equation 13 can be reduced to

$$\Delta p^n + a_1^n \sqrt{|\Delta p^n|}\,\mathrm{sign}(\Delta p^n) + a_2^n = a_3^n u_\mathrm{in}^n \tag{15}$$

where the coefficients $a_1^n \geq 0$, a_2^n and $a_3^n \geq 0$ will depend on known (previously computed) values of y^n and the various defining parameters of the reed system. (The non-negativity of a_1^n and a_3^n, follows from the use of semi-implicit discretizations to the stiffness terms.)

Using the conditions in Equation 14 and the update of Equation 11, as well as Equation 13b, one can arrive at the relation

$$p_\Delta^n = b_1^n - b_2^n u_\mathrm{in}^n \tag{16}$$

where again, b_1^n and $b_2^n \geq 0$ depend on previously computed values of the grid functions p and u, as well as the input pressure p_m. Now, Equations 15 and 16 can be combined into a single equation for the pressure difference p_Δ^n:

$$|p_\Delta^n| + c_1^n \sqrt{|p_\Delta^n|} + \frac{c_2^n}{\mathrm{sign}\,(p_\Delta^n)} = 0 \tag{17}$$

for the coefficents $c_1^n \geq 0$ and c_2^n. One can then observe that, for a solution to exist, one must have $\mathrm{sign}(p_\Delta^n) = -\mathrm{sign}(c_2^n)$, at which point the magnitude $|p_\Delta^n|$ can be determined uniquely. In this case, owing to the form of the pressure-flow characteristic, this can be done using the quadratic formula, but a unique solution will exist for any such characteristic that is one-to-one, though an iterative method (necessarily convergent) may be necessary. In this sense, finite difference updating is simpler here than in the closely related case of the bow-string interaction (in which case the nonlinear force-velocity characteristic is not necessarily one-to-one; Bilbao 2009).

Numerical Radiation Condition

For the scheme at the radiating termination, a discrete condition corresponding to Equation 9 is

$$\frac{1}{2h}\left(\Psi_{N+1}^n - \Psi_{N-1}^n\right) = -\frac{\alpha_1}{2k}\left(\Psi_N^{n+1} - \Psi_N^{n-1}\right) - \frac{\alpha_2}{2}\left(\Psi_N^{n+1} + \Psi_N^{n-1}\right)$$

When this condition is employed in the scheme of Equation 11, the following specialized recursion at the boundary point at $l = N$ results:

$$\Psi_N^{n+1} = m_N^{(-)} \Psi_{N-1}^n + m_N^{(0)} \Psi_N^n + q_N \Psi_N^{n-1} \tag{18}$$

where

$$m_N^{(-)} = \frac{\lambda^2}{2\tau}(S_{N+1} + 2S_N + S_{N-1})$$

$$m_N^{(0)} = \frac{1}{\tau}\left(2 - \frac{\lambda^2}{2}(S_{N+1} + 2S_N + S_{N-1})\right)$$

$$q_N = \frac{1}{\tau}\left(\frac{\gamma^2 k^2}{2h}(S_{N+1} + S_N)\left(\frac{\alpha_1}{k} - \alpha_2\right) - 1\right)$$

and where

$$\tau = \frac{\gamma^2 k^2}{2h}(S_{N+1} + S_N)\left(\frac{\alpha_1}{k} + \alpha_2\right) + 1$$

Explicit Updating

It is important to point out that, despite the apparently complex relationship among the stored variables at the terminations and the grid function to be updated over the interior, a purely explicit update form can be arrived at, but the order in which operations are performed is of great importance. Consider the entire scheme at the end of an update cycle, at which point all values at time step n or previously are known. One can then proceed as follows. First, calculate p_Δ^n through the solution of Equation 17. Next, calculate y^{n+1} through Equation 13a, and calculate p_{in}^n using Equation 13b and the known value of p_{m}^n. Then, calculate $\delta_{t\cdot}\Psi_0^n$, and thus Ψ_0^{n+1} using the first of the boundary conditions of Equation 14. Finally, calculate the remaining values of Ψ_l^{n+1}, $l > 0$ using the schemes in Equations 11 and 18.

At this point, the updating cycle is complete, and the procedure can be repeated. Proponents of wave digital filtering often call attention to this computability issue, usually dealt with using so-called reflection-free ports (Fettweis 1986). One can see here that the same property is available using finite difference schemes, and furthermore, numerical solution uniqueness may be ensured (in contrast with wave digital methods making use of nonlinear elements, and power-normalized waves (Bilbao 2004), where implicit solvers will be necessary) (see Figure 5).

Numerical Stability

The question of numerical stability of the simulation as a whole is a very delicate one. One can prove, using energy techniques (Bilbao 2009), that in the absence of the reed model, the scheme of Equation 11, coupled with the numerical radiation boundary condition in Equation 14, is numerically stable, as long as the condition of Equation 12 is satisfied.

When the reed model is introduced, however, the situation becomes much more complicated—though for many types of nonlinear systems, including schemes for bow-string interactions, and for nonlinear vibrations of strings and plates, one can develop solid stability conditions, the reed system presents some difficulties. The problem is the following: As a starting point, one would like to be able to bound some measure of the size of the state of the continuous model system (i.e., the reed coupled to the bore) in terms of the input signal $p_m(t)$. This is a natural requirement, and one which, in this case, is not met; it is difficult to show that there do not exist bounded input signals which are capable of producing unbounded output. This indicates the possibility that model of reed vibration presented here might not be fully correct, from an energetic standpoint. As such, it may not be possible to find a stability condition for the derived numerical scheme. On the other hand, it is rather difficult to actually exhibit any instability in the scheme proposed here; the author has tried, using the most perverse settings imaginable for the system parameters and input signal!

Computational Considerations

The computational cost of this algorithm is almost entirely due to the updating of the scheme for the tube, and, as such, is governed by the choice of time step k and grid spacing h, which are related by the CFL condition (Equation 12). The condition should be fulfilled as close to equality as possible—otherwise, as mentioned previously, excessive numerical dispersion, leading to mode mistuning and a severe limitation in audio bandwidth (Bilbao 2009) will result. Thus, for a given time step $k = 1/f_s$, the memory requirement will be almost exactly $2f_s/\gamma = 2f_sL/c$ units. Updating at a single grid

point requires three arithmetic operations, and thus the total operation count will be $6f_s^2/\gamma = 6Lf_s^2/c$ operations/second. For typical wind instruments, and at a suitably high audio sample rate, such as $f_s = 44100$ Hz, the operation count will be on the order of tens of megaoperations/second, well within real time capability on a modest laptop computer. For example, on the author's laptop, a Dell with a 2.0 GHz Pentium processor, and for the case of a clarinet geometry, it takes approximately 3.9 sec to generate 5 sec of sound output, at 44.1 kHz, in Matlab—and sluggish Matlab code generally runs between 10 and 100 times slower than a standard C implementation. On the other hand, a finite-difference (FD) implementation is more expensive, in terms of arithmetic (though not memory), than a typical waveguide algorithm.

Tonehole Modeling

In the literature, the tonehole is usually modeled as a branched side-tube, characterized as a two- or three-port lumped circuit element. The reader is referred to the ample literature on this subject (e.g., Keefe 1982a, 1982b). Normally, such an element is described in terms of series and shunt impedances, which depend on the hole radius and effective tonehole height (which depends on the state of the hole), and the enclosed volume.

It is, of course, possible to describe the behaviour of such an element directly in the time-space domain, by adding extra terms to Webster's equation. Here is one very simple variety, written in terms of dimensionless variables, which is equivalent to the lossless form given in van Walstijn and Scavone (2000):

$$S\Psi_{tt} = \gamma^2 (S\Psi_x)_x - \delta(x - x_\mathrm{T})g \tag{19a}$$

$$g = \frac{\phi\gamma^2 S_\mathrm{T}}{\xi_\mathrm{e}}\Psi(x_\mathrm{T}) + (1-\phi)\xi S_\mathrm{T}\Psi_{tt}(x_\mathrm{T}) \tag{19b}$$

Here, ξ is the dimensionless ratio of the tonehole height to the tube physical tube length L, and S_T is the dimensionless ratio of the tonehole cross-sectional area to the area of the bore at its left end (not at the hole!). ϕ is a parameter which indicates the state of tonehole, ranging between $\phi = 0$ (closed) and $\phi = 1$ (open). The various forms for ξ, which depend on whether the hole is opened or closed, are effective lengths, and exact expressions appear in various publications (Keefe 1982a, 1990; van Walstijn and Scavone 2000). In fact, the effective lengths themselves are frequency-dependent to a slight degree. Such frequency dependence, as well as loss due to radiation (Ducasse 2003) is ignored here, for the sake of simplicity (but can easily be reintroduced; Bilbao 2009). The lumped variable $g = g(t)$ is a variable used to store the additional state of the tonehole.

This model is simplified from the usual form seen in the literature (Keefe 1982a), which, when viewed as a two-port lumped circuit element, contains negative impedances (leading to the so-called negative length correction). Such negative elements can indeed be incorporated into the framework above (Bilbao 2009), but at the risk of introducing numerically unstable behaviour, which is not surprising, given that such elements cannot be interpreted as passive.

In an FD implementation, the coupling with the tone-hole model can carried out using some form of interpolation (i.e., the tonehole location will not, in general, fall directly at one of the grid locations). Here is a general form:

$$\Psi_l^{n+1} = m_l^{(-)}\Psi_{l-1}^n + m_l^{(0)}\Psi_l^n + m_l^{(+)}\Psi_{l+1}^n - \Psi_l^{n-1} - \frac{4k^2}{S_{l-1} + 2S_l + S_{l+1}} J_l(x_\mathrm{T}) g^n$$

$$g^n = \frac{\phi\gamma^2 S_\mathrm{T}}{2\xi_\mathrm{e}}(\Psi^{n+1}(x_\mathrm{T}) + \Psi^{n-1}(x_\mathrm{T})) + \frac{(1-\phi)\xi S_\mathrm{T}}{k^2}(\Psi^{n+1}(x_\mathrm{T}) - 2\Psi^n(x_\mathrm{T}) + \Psi^{n-1}(x_\mathrm{T}))$$

Here, $\Psi^n(x_\mathrm{T})$ is an interpolated value drawn from the grid function Ψ_l^n; if linear interpolation is used, for example, $\Psi^n(x_\mathrm{T}) = \alpha\Psi_{l_\mathrm{T}}^n + (1-\alpha)\Psi_{l_\mathrm{T}+1}^n$, where the interpolation point x_T lies between the grid locations $l = l_\mathrm{T}$ and $l = l_\mathrm{T} + 1$, and where $0 \le \alpha < 1$ is an interpolation index. Similarly, the grid function $J_l(x_\mathrm{T})$ is an approximation to a delta function centered at x_T, and when linear interpolation is used, takes on the values $J_{l_\mathrm{T}} = \alpha/h$, $J_{l_\mathrm{T}+1} = (1-\alpha)/h$, and is zero otherwise.

Figure 5. Typical output spectra for various bore types: (a) a cylinder, (b) a cylinder with a clarinet-like bell, and (c) a cylinder with a bell of extreme flare. In each case, the other model parameters correspond, roughly, to those of a clarinet: $\gamma = 512$, $\mathcal{Q} = 1.6 \times 10^{10}$, $\mathcal{R} = 0.032$, $\mathcal{S} = 10^{-6}$, $\omega_0 = 23250$, $\mathrm{g} = 3000$. The scheme of Equation 11 is used, at a sample rate of 44.1 kHz.

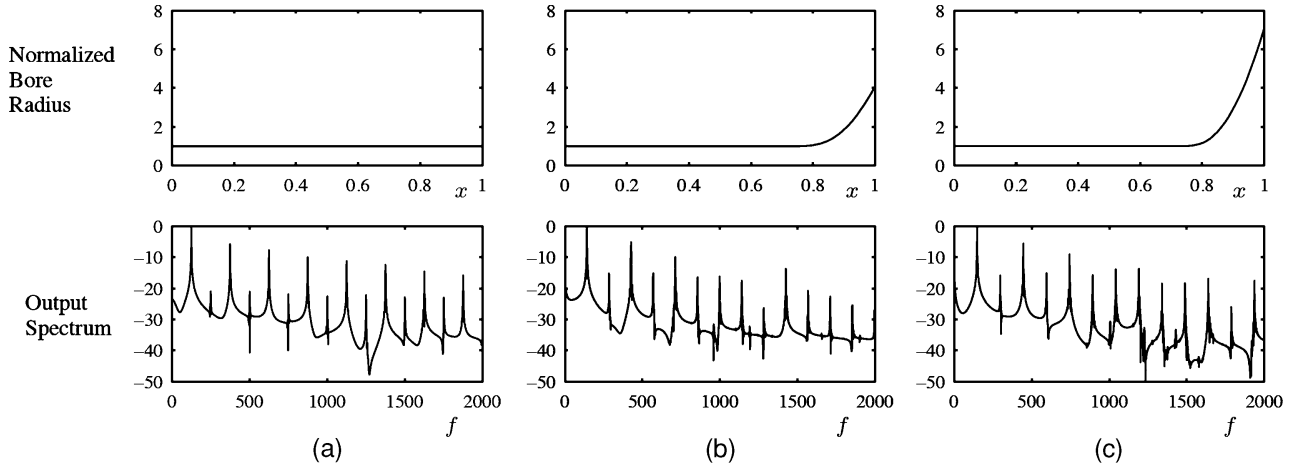

Figure 5

Obviously, the interpolation and delta-function approximation could be extended to a higher order, but linear approximation is probably sufficient. Interestingly, if the interpolation and delta-function approximation are of the same order, one can prove numerical stability of the combined tube/tonehole system, under static conditions (Bilbao 2009). Though this scheme apparently is implicit, it is possible to arrive at an explicit update, much in the same way as for the radiation termination (Bilbao 2009).

Simulation Results

This FD model successfully replicates many features of acoustic reed wind instruments (and also of other synthesis methods), and a variety of such features are presented here. Sound examples are available at the author's Web site, at http://ccrma.stanford.edu/~bilbao/soundex/reed.

Bore Profiles

It is particularly simple, in the direct FD framework, to alter the bore profile: The function $S(x)$ can be set arbitrarily, and, once set, values of the function are used, without further calculations (as of scattering coefficients or impedances) in the simulation. It is thus straightforward to experiment with bore profiles that differ substantially from, for example, those that lead to efficient waveguide realizations (see Figure 5). One must beware, however, that for extreme variations in the cross-sectional area, Webster's equation itself fails to be a good model of the tube dynamics. In particular, computational effort is independent of the choice of bore profile.

Figure 6. Non-dimensional reed displacement y*, for a clarinetlike configuration, of parameters as given in the caption to Figure 5, and with a bore profile as shown in Figure 5b. The parameters for the collision term in Equation 4 are chosen as $\omega_1 = 632$, and the nonlinearity exponent is $\alpha = 4$. In (a), the input is a steady nondimensional mouth pressure of $\mathrm{p_m} = 0.013$, and in (b), $\mathrm{p_m} = 0.02$.*

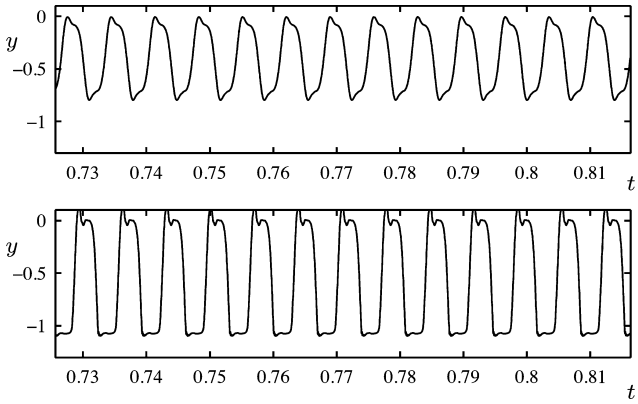

Figure 6

Reed Beating

As an example of typical phenomena generated by such a model, consider the perceptually important reed-beating effect, as illustrated in Figure 6. In

Figure 7. Non-dimensional output pressure, for the wind model of parameters given in the caption to Figure 5, and using the clarinet-like bore profile shown in Figure 5b. Top, with a nondimensional mouth pressure of $p_m = 0.0134$*, center, with* $p_m = 0.0148$*, and bottom, with* $p_m = 0.0168$*.*

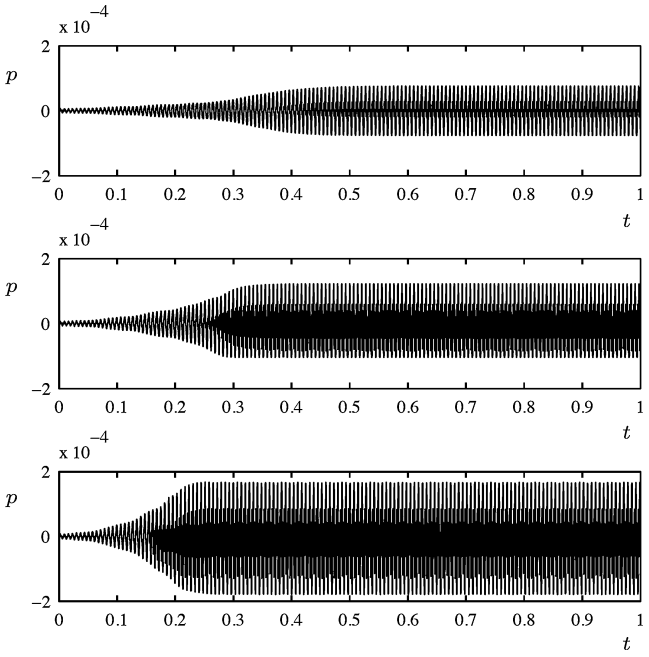

particular, note that the nondimensional reed displacement takes on values < -1; the extent of such "penetration" may be controlled through the choice of ω_1 and α, but the general results are in agreement with other published results (see, e.g., Keefe 1992).

Onset Times

As another example, the variation in onset times for notes as a function of mouth pressure, characteristic of wind instruments, is shown in Figure 7.

Time Variations in the Equilibrium Reed Displacement

When the equilibrium reed displacement H_0 is allowed to vary slightly, and at sub-audio rates (as in a typical wind instrument gesture), variations in timbre result (see Figure 8).

Figure 8. Top: relative variation in reed equilibrium displacement $H(t)/H_0$*. Middle: output pressure waveform (non-dimensional), and bottom, its spectrogram. The model is of parameters as described in the caption to Figure 5, and the input waveform is a constant with* $p_m = 0.013$*. The scheme of Equation 11 is used, at a sample rate of 48 kHz.*

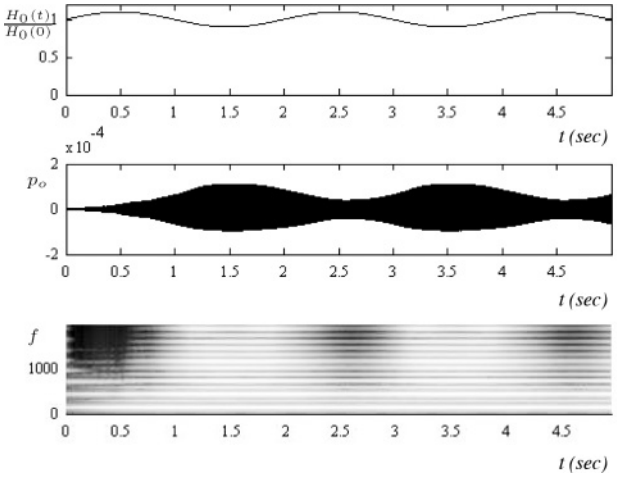

Tonehole Openings

Like other physical modeling synthesis methods, the FD tonehole model presented here allows for changes in pitch, through time variation in the parameter ϕ, which specifies a state between open and closed (see Figure 9), which is generated using a saxophone-like model, with a series of toneholes.

Squeaks and Multiphonics

A variety of multiphonics can be generated though judicious placement of toneholes. If, for instance, a single tonehole is opened a good distance away from the bell, one is likely to generate a sound with a multiphonic character, exhibiting, perhaps, distinct sounding pitches, and a sub-audio rate time-varying amplitude envelope (see Figure 10), illustrating such a "warbling" effect. The space of such sounds, as any wind player will know, is very large indeed, and will depend on mouth pressure, the rate at which the hole is opened or closed, in addition to the particulars of tonehole placement and geometry.

Conclusion

Perhaps the greatest advantage of a fully discrete formulation is fidelity to the physics of the continuous

Figure 9. Spectrogram of output pressure for a gesture in an instrument of conical bore. Five toneholes are tuned approximately to a minor scale.

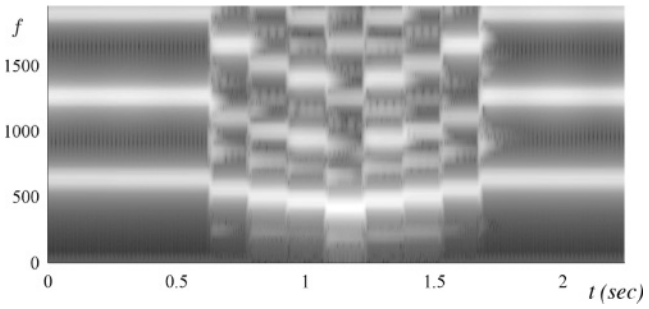

Figure 10. Spectrogram of output pressure, for the wind model of parameters given in the caption to Figure 5, and using the clarinet-like bore profile shown in Figure 5b, with a tonehole located at $x_T = 0.6$*, with parameters* $S_T = 0.1644$*,* $\xi = 0.0075$*, and* $\xi_e = 0.0134$*. The tonehole is opened, over a duration of 10 msec, at time* $t = 1$ *sec.*

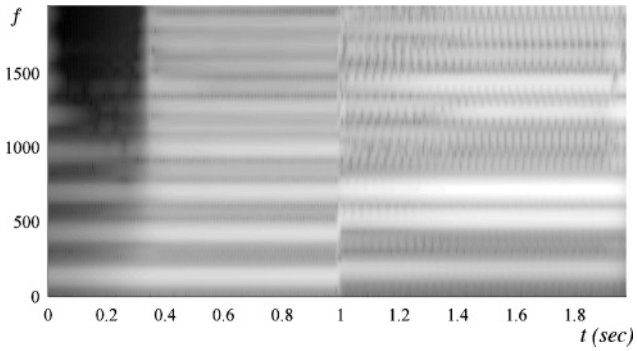

time/space model itself; as a result, many issues that appear in more efficient designs, such as "lumping" of impedances, fractional delay interpolation, etc., can be sidestepped. Another advantage is extensibility; see subsequently for some examples. The greatest disadvantage is computational cost, which is, in fact, quite small by today's standards, though certainly higher than that of, say, a waveguide model.

There are many ways in which the FD wind model here could be extended. Several are in progress and have not been discussed in this short article. In particular, there is a simple extension to "blown open" brass-like instruments that is nearly trivial, involving only a single change in polarity of the pressure difference Δp in the model. Another obvious step is the porting of such an algorithm to a real-time environment such as Max/MSP (Zicarelli 2002) or Csound (Boulanger 2001). As noted earlier, a real-time implementation is easily possible, and such developments are under way.

Other extensions are also possible. The fully discrete FD approach is very well suited to an extension to nonlinear one-dimensional wave propagation; the linearity hypothesis is probably sufficient for reed instruments and brass instruments under moderate amplitude excitation, though nonlinear effects do appear at high amplitudes in instruments such as the trombone (Hirschberg et al. 1996), and have indeed been modeled in synthesis applications (Mmsallam et al. 2000; Vergez and Rodet 2000). Fully discrete methods in computing shock wave solutions have a long history in mainstream fluid dynamics applications (e.g., Sod 1978; Hirsch 1988; Leveque 2002), which is concerned with finite-volume methods in the context of nonlinear fluid-dynamics applications. The introduction of loss in the acoustic tube, however, is in some ways more problematic. Often, loss in the boundary layer of a tube is modeled in the frequency domain; when transformed back to the time domain, one arrives at a partial differential equation involving fractional derivatives, which can cause immense difficulty numerically. However, discrete models of loss have been examined in great detail, in the scattering context, by various authors (e.g., Hélie and Matignon 2006).

Finally, the model described here is generally valid when bore radius is small compared to audio wavelengths, and when its spatial variation is not too great. In other cases, one might need to resort to models of wave propagation incorporating higher modes, and possibly mode conversion. In the fully discrete case, one could employ a three-dimensional model of the tube, with a coarse grid approximation in the transverse direction (Noreland 2002), though one must beware the effects of numerical dispersion, which can be extreme in coordinate systems other than Cartesian.

References

Atig, M., J.-P. Dalmont, and J. Gilbert. 2004. "Termination Impedance of Open-Ended Cylindrical Tubes at High Sound Pressure Level." *Comptes Rendus Mécanique* 332:299–304.

Avanzini, F., and D. Rocchesso. 2002. "Efficiency, Accuracy, and Stability Issues in Discrete Time Simulations of Single Reed Instruments." *Journal of the Acoustical Society of America* 111(5):2293–2301.

Avanzini, F., and M. van Walstijn. 2004. "The Mechanical Response of the Reed-Mouthpiece-Lip System of a Clarinet. Part I: A One-Dimensional Distributed Model." *Acta Acustica United with Acustica* 90(3):537–547.

Backus, J. 1963. "Small Vibration Theory of the Clarinet." *Journal of the Acoustical Society of America* 35(3):305–313.

Belevitch, V. 1968. *Classical Network Theory*. San Francisco, California: Holden Day.

Benade, A., and E. Jansson. 1974. "On Plane and Spherical Waves in Horns with Nonuniform Flare I: Theory of Radiation, Resonance Frequencies, and Mode Conversion." *Acustica* 31(2):80–98.

Bilbao, S. 2004. *Wave and Scattering Methods for Numerical Simulation*. Chichester, UK: Wiley.

Bilbao, S. 2008. "Direct Simulation for Wind Instrument Synthesis." *Proceedings of the 11th International Digital Audio Effects Conference.* Espoo, Finland: Helsinki University of Technology, pp. 145–152.

Bilbao, S. 2009. *Numerical Sound Synthesis: Finite Difference Schemes and Simulation in Musical Acoustics.* Chichester, UK: Wiley.

Bilbao, S., J. Bensa, and R. Kronland-Martinet. 2003. "The Wave Digital Reed: A Passive Formulation." *Proceedings of the COST-G6 Digital Audio Effects Conference.* London: Queen Mary, University of London, pp. 225–230.

Boulanger, R., ed. 2001. *The Csound Book: Perspectives in Software Synthesis, Sound Design, Signal Processing, and Programming.* Cambridge, Massachusetts: MIT Press.

Chaigne, A., and A. Askenfelt. 1994. "Numerical Simulations of Struck Strings I: A Physical Model for a Struck String Using Finite Difference Methods." *Journal of the Acoustical Society of America* 95(2):1112–1118.

Courant, R., K. Friedrichs, and H. Lewy. 1928. "Über die partiellen Differenzengleichungen de mathematischen Physik." *Mathematische Annalen* 100:32–74.

Dalmont, J.-P., J. Gilbert, and S. Ollivier. 2003. "Nonlinear Characteristics of Single-Reed Instruments: Quasistatic Volume Flow and Reed Opening Characteristics." *Journal of the Acoustical Society of America* 114(4):2253–2262.

Ducasse, E. 2003. "A Physical Model of a Single Reed Wind Instrument, Including Actions of the Player." *Computer Music Journal* 27(1):59–70.

Fettweis, A. 1986. "Wave Digital Filters: Theory and Practice." *Proceedings of the IEEE* 74(2):270–327.

Fletcher, N., and T. Rossing. 1991. *The Physics of Musical Instruments.* New York: Springer-Verlag.

Guillemain, P. 2004. "A Digital Synthesis Model of Double-Reed Wind Instruments." *EURASIP Journal of Applied Signal Processing* 7:990–1000.

Hélie, T., and D. Matignon. 2006. "Diffusive Representations for the Analysis and Simulation of Flared Acoustic Pipes with Viscothermal Losses." *Mathematical Models and Methods in Applied Sciences* 16(4):503–536.

Hirsch, C. 1988. *Numerical Computation of Internal and External Flows.* Chichester, UK: Wiley.

Hirschberg, A., et al. 1996. "Shock Waves in Trombones." *Journal of the Acoustical Society of America* 99(3):1754–1758.

Keefe, D. 1982a. "Theory of the Single Woodwind Tone Hole." *Journal of the Acoustical Society of America* 72(3):676–687.

Keefe, D. 1982b. "Experiments on the Single Woodwind Tone Hole." *Journal of the Acoustical Society of America* 72(3):688–699.

Keefe, D. 1990. "Woodwind Air Column Models." *Journal of the Acoustical Society of America* 88(1):35–51.

Keefe, D. 1992. "Physical Modeling of Wind Instruments." *Computer Music Journal* 16(4):57–73.

Kelly, J., and C. Lochbaum. 1962. "Speech Synthesis." *Proceedings of the Fourth International Congress on Acoustics.* Copenhagen: International Acoustics Commission, pp. 1–4.

Kergomard, J. 1995. "Elementary Considerations on Reed Instrument Oscillations." In A. Hirschberg, J. Kergomard, and G. Weinreich, eds. *Mechanics of Musical Instruments.* New York: Springer, pp. 229–290.

Kergomard, J., P. Guillemain, and T. Voinier. 2005. "Real-Time Synthesis of Clarinet-Like Instruments Using Digital Impedance Models." *Journal of the Acoustical Society of America* 118(1):483–494.

Leveque, R. 2002. *Finite Volume Methods for Hyperbolic Problems.* Cambridge, UK: Cambridge University Press.

McIntyre, M., R. Schumacher, and J. Woodhouse. 1983. "On the Oscillations of Musical Instruments." *Journal of the Acoustical Society of America* 74(5):1325–1345.

Morse, P., and U. Ingard. 1968. *Theoretical Acoustics.* Princeton, New Jersey: Princeton University Press.

Msallam, R., et al. 2000. "Physical Model of the Trombone Including Nonlinear Propagation Effects: Application to the Sound Synthesis of Loud Tones." *Acta Acustica United with Acustica* 86:725–736.

Nederveen, C. 1998. "Influence of a Toroidal Bend on Wind Instrument Tuning." *Journal of the Acoustical Society of America* 104(3):1616–1626.

Noreland, D. 2002. "A Numerical Method for Acoustic Waves in Horns." *Acta Acustica United with Acustica* 88(4):576–586.

Portnoff, M. 1973. "A Quasi-One-Dimensional Digital Simulation for the Time-Varying Vocal Tract." MS Thesis, Massachusetts Institute of Technology.
Rabiner, L., and R. Schafer. 1978. *Digital Processing of Speech Signals.* Englewood Cliffs, New Jersey: Prentice-Hall.
Scavone, G. 1997. "An Acoustic Analysis of Single-Reed Woodwind Instruments with an Emphasis on Design and Performance Issues and Digital Waveguide Techniques." PhD Dissertation, Department of Music, Stanford University.
Shubin, G. R., and J. B. Bell. 1987. "A Modified Equation Approach to Constructing Fourth Order Methods for Acoustic Wave Propagation." *SIAM Journal of Scientific and Statistical Computing* 8:135–151.
Smith, J. O., III. 1986. "Efficient Simulation of the Reed-Bore and Bow-String Mechanisms." *Proceedings of the 1986 International Computer Music Conference.* San Francisco, California: International Computer Music Association, pp. 275–280.
Sod, G. 1978. "A Survey of Several Finite Difference Methods for Systems of Nonlinear Hyperbolic Conservation Laws." *Journal of Computational Physics* 27(1):1–31.
Strikwerda, J. 1989. *Finite Difference Schemes and Partial Differential Equations.* Pacific Grove, California: Wadsworth and Brooks/Cole Advanced Books and Software.
Tachibana, T., and K. Takahashi. 2000. "Sounding Mechanism of a Cylindrical Pipe Fitted with a Clarinet Mouthpiece." *Progress of Theoretical Physics* 104(2): 265–288.
Välimäki, V., and M. Karjalainen. 1995. "Implementation of Fractional Delay Waveguide Models Using Allpass Filters." *Proceedings of the 1995 IEEE International Conference on Acoustics, Speech, and Signal Processing.* Piscataway, New Jersey: Institute of Electrical and Electronics Engineers, pp. 8–12.
van den Doel, K., and U. Ascher. 2008. "Real-Time Numerical Solution of Webster's Equation on a Non-Uniform Grid." *IEEE Transactions on Audio, Speech and Language Processing* 16(6):1163–1172.
van Walstijn, M. 2007. "Wave-Based Simulation of Wind Instrument Resonators." *IEEE Signal Processing Magazine* 24(2):21–31.
van Walstijn, M., and F. Avanzini. 2007. "Modeling the Mechanical Response of the Reed-Mouthpiece-Lip System of a Clarinet. Part II: A Lumped Model Approximation." *Acta Acustica United with Acustica* 93(3):435–446.
van Walstijn, M., and D. Campbell. 2003. "Discrete-Time Modeling of Woodwind Instrument Bores Using Wave Variables." *Journal of the Acoustical Society of America* 113(1):575–585.
van Walstijn, M., and G. Scavone. 2000. "The Wave Digital Tonehole Model." *Proceedings of the 2000 International Computer Music Conference.* San Francisco, California: International Computer Music Assocaition, pp. 465–468.
Vergez, C., and X. Rodet. 2000. "A New Algorithm for Nonlinear Propagation of Sound Waves: Application to a Physical Model of a Trumpet." *Journal of Signal Processing* 4:79–88.
Zicarelli, D. 2002. "How I Learned to Love a Program That Does Nothing." *Computer Music Journal* 26(4):44–51.